Separation of platelets from other blood cells in continuous-flow by dielectrophoresis field-flow-fractionation

Niccolò Piacentini,[1,a),b)] Guillaume Mernier,[2,a)] Raphaël Tornay,[2] and Philippe Renaud[2]
[1]*Dipartimento di Elettronica, Politecnico di Torino, Corso Duca degli Abruzzi 24, 10129 Torino, Italy*
[2]*Microsystems Laboratory, École Polytechnique Fédérale de Lausanne (EPFL), Station 17, Lausanne, Vaud 1015, Switzerland*

(Received 12 July 2011; accepted 24 August 2011; published online 21 September 2011)

We present a microfluidic device capable of separating platelets from other blood cells in continuous flow using dielectrophoresis field-flow-fractionation. The use of hydrodynamic focusing in combination with the application of a dielectrophoretic force allows the separation of platelets from red blood cells due to their size difference. The theoretical cell trajectory has been calculated by numerical simulations of the electrical field and flow speed, and is in agreement with the experimental results. The proposed device uses the so-called "liquid electrodes" design and can be used with low applied voltages, as low as 10 V_{pp}. The obtained separation is very efficient, the device being able to achieve a very high purity of platelets of 98.8% with less than 2% cell loss. Its low-voltage operation makes it particularly suitable for point-of-care applications. It could further be used for the separation of other cell types based on their size difference, as well as in combination with other sorting techniques to separate multiple cell populations from each other. © *2011 American Institute of Physics*. [doi:10.1063/1.3640045]

I. INTRODUCTION

Platelets are cell fragments present in the blood and involved in the hemostasis. Disorders arising from abnormal platelet concentration can pose serious threats to health. Low platelet concentration can cause hemorrhaging, whereas high concentration can lead to thrombosis and related complications such as infarction, embolism or stroke.[1] It is therefore essential to monitor the platelet concentration to diagnose such deviations early enough for appropriate treatment. Besides this diagnostics need, there is also a demand for platelet sample preparation in applications such as transfusion or medical research. To date, several techniques have been used for such separation, including centrifugation,[2] mechanical filtering,[3] and antibody recognition.[4] All these techniques have to face challenges related to the cell size (platelets: 2–3 μm and red blood cells: 7–8 μm), the relatively low concentration of platelets compared to red blood cells (2×10^8 platelets/ml versus 5×10^9 red blood cells/ml) and possible activation of the platelets during handling. Recently, Pommer *et al*. showed the possibility to use dielectrophoresis for platelet separation from blood using a double-stage miniaturized system, requiring the use of high voltages (100 V).[5]

This paper reports on a setup able to separate platelets from blood using a single-stage, low-voltage system combining microchannels in H-filter configuration and dielectrophoresis (DEP) to achieve dielectrophoresis field-flow-fractionation (DEP-FFF). Previous work from our group showed dielectrophoretic separation of cells by differences in dielectric properties, such

[a)]These authors contributed equally to this work.
[b)]Author to whom correspondence should be addressed. Electronic mail: niccolo.piacentini@polito.it.

as living and dead yeast cells.[6] This sorting technique used a parameter of the cells called "opacity," which is the ratio between the values of the Clausius-Mossotti factor at two different frequencies. However, the dependence of dielectrophoretic force on the cell size makes sorting cells with large size differences in an opacity-based system a challenge. DEP-FFF allows overcoming this limitation and has been used in this work to separate cells depending on their size, using significantly lower voltages than the state-of-the-art. The proposed system uses a buffer flow to focus the cell on one side of the main channel, from which the dielectrophoretic force selectively repels the biggest cells in a stronger manner due to the proportionality of the force with the cell volume. In the context of blood sorting, the platelets are the smallest cells in the blood and are deviated much less than bigger cells such as red and white blood cells. A bifurcation situated after the sorting region separates the cells according to their position in the flow stream. Besides achieving high purity and recovery rates, this device could easily integrate other techniques, seamlessly sharing the technological platform, such as opacity-based cell sorting,[6] cell coulter counting,[7,8] or cell lysis,[9,10] and could be applied in point-of-care applications such as detection of platelet loss during chemotherapy.[11]

II. MATERIALS AND METHODS

A. Chip design, fabrication and packaging

The device used in this work is similar to a device used previously for the functionalization of nanoparticles.[12] The fabrication process is described elsewhere[13] and shortly repeated here. The device is made on a 4-in. glass substrate with a thickness of 525 μm. Two hundred nanometer thick platinum electrodes are sputtered on top of a 20 nm-thick titanium adhesion layer, and further patterned by lift-off. The microchannels are made using a 40 μm-high SU8 layer and the wafer is diced in 20 mm $\times$ 15 mm chips. The obtained chips are placed on a chip holder made in acrylic, and connected to a printed circuit board taking care of the signal amplification and of the distribution to the appropriate contacts. A polydimethylsiloxane (PDMS) block is placed on top of the chip to seal the microchannels and is mechanically fixated using a plastic piece. The setup allows access to the fluidic inlets and outlets, and pressure regulation with a pressure setup as described previously by Braschler *et al.*[14]

The chip design includes three different parts: an injection region, a separation region and a collection region, as depicted in Figure 1. By convention, the "left" and "right" sides of the channel are taken as the direction the cells see while flowing. A mixture of blood cells is injected at the left inlet and buffer comes from the right inlet. Due to the small channel dimensions (only 40 μm in width), the flow is laminar in the separation region (Reynolds number < 0.05) so that the two flows do not mix. The device uses the so-called "liquid electrodes," which are planar electrodes patterned at the bottom of dead-end chambers positioned perpendicularly to the main channel, as defined by Demierre *et al.*[15] They provide a homogeneous electrical field over the total channel height while keeping a simple process flow with a single planar metal layer. Dielectrophoresis signals are applied on liquid electrodes placed on the left side of the channel as described by Tornay *et al.*[12] The dielectrophoretic force repels the bigger

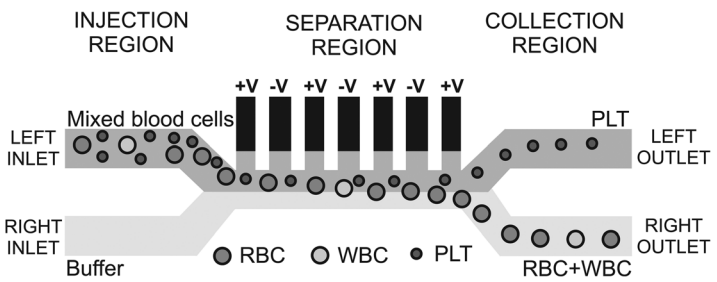

FIG. 1. Schematic of the chip design, showing the different regions and the behavior of the PLTs, RBCs, and WBCs in the system. The microfluidic channels are 40 μm high and 40 μm wide. The dielectrophoretic voltage is applied on the "liquid electrodes" placed on the left side of the channel in the separation region.

red blood cells (RBCs) and white blood cells (WBCs) which go out at the right channel, whereas the smaller platelets (PLTs) are not deviated enough and are collected at the left channel.

The chip design ensures a minimal exposure of platelets to materials capable of eventually activating them. PDMS is known to be nonthrombogenic,[16] and the lower hemocompatibility of SU-8 and, to a smaller extent, of glass[17] is compensated by the use of a strong and reversible anticoagulant, as described in Sec. II B. Moreover, the on-chip permanence time of cells (less than 1 min) is significatively shorter than any time causing activation, which has been reported in literature.[17] Finally, our "liquid electrodes" intrinsically protect cells from coming into contact with metal and being exposed to high electrical fields.

B. Protocols

The working solution is phosphate buffer saline (PBS) diluted in sucrose solution to reach the conductivity of 55 mS/m while keeping an osmolarity of 300 mOsm/l. The addition of 1% w/v bovine serum albumin (BSA) reduces the adhesion of cells on the microchannel walls. Whole blood is obtained from a healthy donor and collected in a tube containing disodium ethylenediaminetetraacetic acid (K_2EDTA, 1.5 mg/ml of blood) to avoid coagulation. EDTA is a strong and reversible anticoagulant inhibiting the clotting process by removing calcium from the blood[18] without inducing morphological changes in the cells.[19] The blood is then treated as follows to increase the platelets concentration for an easier evaluation of the sorting device. The blood is centrifuged for 5 min at 1000 rpm. The sample on the top of the tube, containing mostly platelets, is remixed with the sample at the bottom at the tube (containing RBCs) and diluted in the working solution to obtain a concentration around $1–2 \times 10^8$ cells per ml for both RBCs and PLTs. WBCs are in very low concentration and can be neglected here. These sample preparation steps are only needed to be able to evaluate the system by video analysis. The system is suitable to work with a blood sample, with an optional dilution that could be done on chip. The sample and buffer are injected by pipetting at the fluidic inlets and the sorting is observed under an inverted microscope (Leica) equipped with a CCD video camera (uEye 2210, IDS Imaging).

III. THEORETICAL CONCEPTS

A. Dielectrophoresis

The dielectrophoretic force is used to separate the cells based on their size. The time average of this force in an inhomogeneous and time-varying electrical field E is proportional to the cell volume, as shown by the following equation:[20,21]

$$\langle F_{DEP}(t)\rangle = 2\pi\varepsilon_m r^3 \mathrm{Re}(K_{CM})\nabla|\mathrm{E_{RMS}}|^2 \tag{1}$$

where ε_m is the permittivity of the medium, r the radius of the particle, and $\mathrm{Re}(K_{CM})$ is the real part of the Clausius-Mossotti factor defined as

$$K_{\mathrm{CM}} = \frac{\underline{\varepsilon}_\mathrm{p} - \underline{\varepsilon}_\mathrm{m}}{\underline{\varepsilon}_\mathrm{p} - 2\underline{\varepsilon}_\mathrm{m}}, \underline{\varepsilon} = \varepsilon - \mathrm{j}\frac{\sigma}{\omega} \tag{2}$$

$\underline{\varepsilon}$ being the complex permittivity taking into account the permittivity ε and the conductivity σ of the particle and the medium; ω is the angular frequency of the electric field, j the imaginary unit. The real part of K_{CM} is bounded between -0.5 and 1, and can give rise to DEP forces in two opposite directions. Namely, one refers to positive dielectrophoresis (pDEP) when cells are attracted in regions where the gradient of electric field is large. Conversely, cells are repelled from those regions in case of negative dielectrophoresis (nDEP). Figure 2 shows the real part of the Clausius-Mossotti factor for red blood cells and platelets.

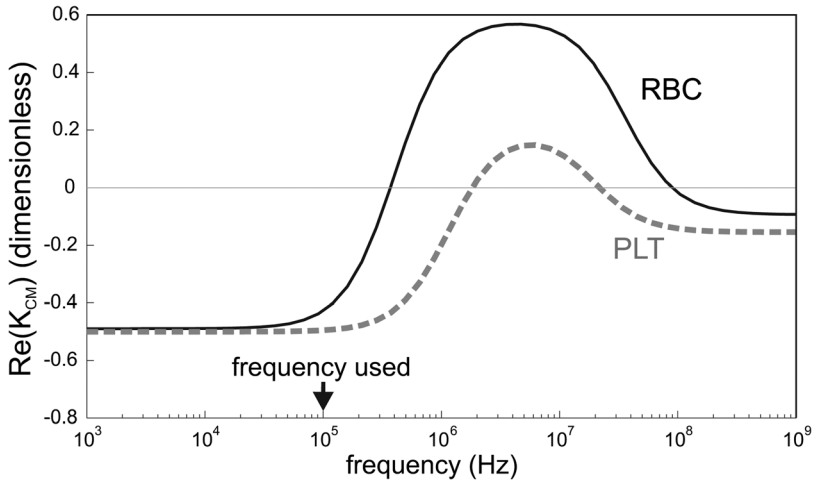

FIG. 2. Real part of the Clausius-Mossotti factor for RBCs and PLTs in a medium with a conductivity of 55 mS/m, using a single-shell model with the parameters found in the literature (Refs. 22 and 23). The curves were obtained using the spherical single shell model described by Gimsa *et al*. (Ref. 24).

In previous works,[6–8] the cell sorting was based on the cell opacity, which is the ratio of the value of the Clausius-Mossotti at different frequencies. However, the small size of the platelets does not allow to use this system as they are not enough deviated. Therefore repulsion by negative dielectrophoresis is used here in combination with hydrodynamic focusing. This technique has also the advantage of only using strong negative dielectrophoresis, which can be performed in any solution conductivity, whereas the opacity-based sorting works best in solutions with low conductivity. By integrating the size-based sorting described here and the previously developed opacity-based sorting, it would be possible to sort cells using both parameters, as it is done in multiple-frequency impedance measurements.[25,26]

The frequency used in this work is 100 kHz where both RBCs and PLTs are experiencing negative dielectrophoresis, but the dielectrophoretic force is much stronger for the RBCs than for the PLTs due to the size difference. The dielectrophoretic force is opposed by the friction of the medium on the cells, giving total force

$$F_{TOT} = F_{DEP} - f\upsilon \tag{3}$$

where υ is the speed of the cells relative to the medium and f is the friction factor given by

$$f = 6\pi\eta r \tag{4}$$

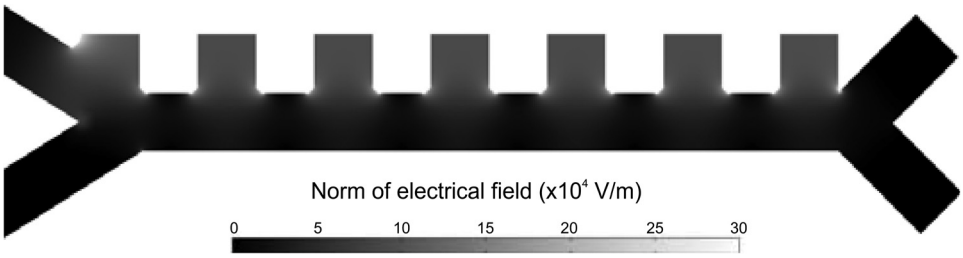

FIG. 3. Electric field intensity map. The represented norm of the electric field is at the origin of the dielectrophoretic repulsion of RBCs away from the electrodes. As it can be seen, the higher gradient regions are located at the corners of the lateral electrode channels, as well as in front of them. Then the cell trajectory builds up as a combination of the hydrodynamic focusing against the electrodes and the dielectrophoretic repulsion towards the lower part of the channel occurring at each electrode pair.

assuming a spherical cell of radius r in a medium of viscosity η. The steady-state velocity of the cell due to dielectrophoresis is obtained when considering a net force on the cell equal to 0, and is given by the magnitude of the DEP force divided by the friction factor,

$$v = \frac{F_{\mathrm{DEP}}}{f} \tag{5}$$

and is therefore proportional to the square of the cell radius. The RBCs have an average volume of 85 fl,[27] whereas the PLT mean volume is around 7–10 fl.[28] The PLTs will therefore experience a DEP force 10 times smaller than the RBCs, and a velocity due to DEP around 5 times smaller.

As the cells considered here have sizes larger than 500 nm, their diffusion in the separation region can be considered to be negligible.[12]

B. Numerical simulations

Numerical simulations are performed to evaluate both convection and dielectrophoretic forces exerted on the cells. Two-dimensional finite element analysis with the software package COMSOL Multiphysics (electrostatics and convection-diffusion modules) returns the distribution of the field and the flow inside the device geometry. Figure 3 shows a map of the norm of the electric field.

The force vectors are obtained by data post-processing using MATLAB (The MathWorks Inc.) and used to calculate the theoretical trajectory of the cells, by adapting the position with the steady-state velocity. Starting from the gradient of the squared electric field and knowing the cell size and Clausius-Mossotti factors, the cell DEP velocity is computed according to Eq. (5) for a given applied voltage. Given a starting position somewhere at the cell inlet, the cell trajectory is then traced by iteratively updating the position according to the flow field and the DEP velocity. Figure 4 shows the obtained theoretical trajectory of the cells inside the device geometry. As it can be seen, it is possible to select a combination of sheath focusing and nDEP such that the RBC is deviated enough to go to the right channel while the PLT stays on the left, thanks to the bifurcation acting as a laminar splitter.

The "stability" of the sorter has also been numerically investigated by analysing the effect of the starting position of the cells on the theoretical trajectory. From the results of the simulations (not shown here), the device is capable of maintaining the sorting performance with output positions varying by small fractions of the cell diameter, as the blood flow is strongly focused on the left side of the channel. The major contribution to a possible spread in output position can thus be ascribed to the effect of the presence of cell clusters.

IV. EXPERIMENTAL RESULTS AND DISCUSSION

The proposed device is used to separate platelets from blood using DEP-FFF. The sample is prepared as described in Sec. II B, and is injected together with PBS in the corresponding

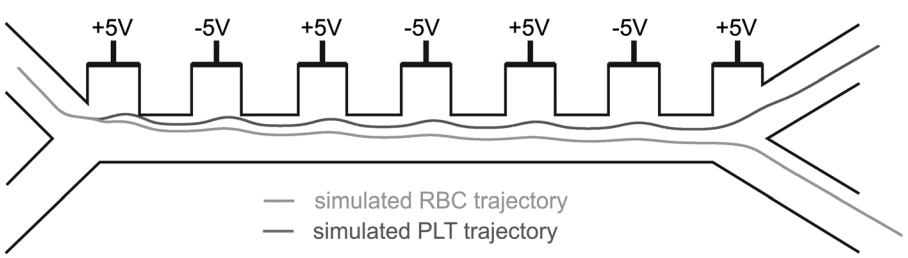

FIG. 4. Theoretical trajectory of the RBCs and PLTs inside the device. The flow speed at the top and bottom inlet is 134 and 853 μm/s, respectively. The voltage applied between neighboring electrodes is 10 V_{pp}. The theoretical value of the Clausius-Mossotti at 100 kHz is used for both cell types (-0.43 and -0.49 for RBCs and PLTs, respectively).

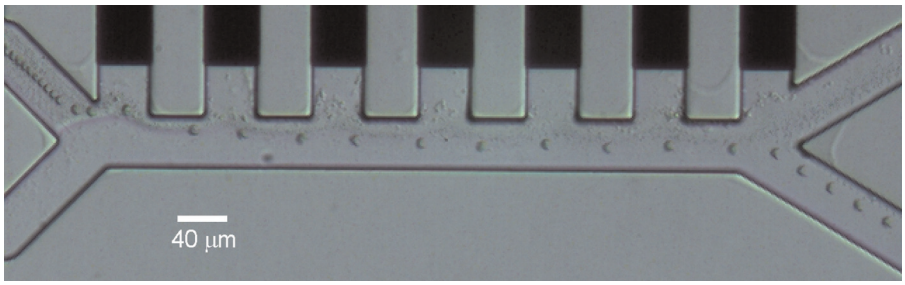

FIG. 5. Trajectory of RBCs and PLTs in the device, obtained by superposition of consecutive video frames. The flow speed at the top and bottom inlet is 134 and 853 μm/s, respectively. The voltage applied between neighboring electrodes is 10 V_{pp} at 100 kHz. For this experiment, the concentration of PLTs was higher than the RBC concentration for better visualization of the trajectory.

inlets. The hydrodynamic focusing is first calibrated by adapting the pressures applied at the inlets to achieve a focusing of the cells on the left side of the channel. The dielectrophoretic voltage is then applied between neighboring liquid electrodes as has been shown in Figure 4.

A first test is performed to validate the operation of the device, using a voltage of 10 V_{pp} at 100 kHz. Figure 5 shows the trajectory of the PLTs and RBCs in the device, obtained by superposition of consecutive frames of a video recorded in the separation region at 20 frames per second with the CCD camera mounted on the microscope. This experiment shows a clear repulsion of the RBCs away from the electrodes due to negative dielectrophoresis, making those big cells exit the separation region in the right channel. The dark trace on the left side shows the trajectory of the PLTs, which are too small to be strongly repelled and stay with the laminar flow on the left side of the channel and exit the separation region on the left collection channel. The concentration of PLTs used in this experiment is higher than the concentration of RBCs to better visualize the platelet trajectory, otherwise difficult to see due to the small PLT size. No WBC was observed due to their small concentration. The flow speed used at the top and bottom inlet is 134 and 853 μm/s, respectively. Cells are focused towards the center at the inlet due to the parabolic flow profile.

This first experiment validates the proof-of-concept of blood cell sorting based on their size and shows that the platelets and red blood cells can be collected in the different channels. This experiment is in good agreement with the simulated trajectory, as it can be seen in Figure 6.

In order to study the robustness of the system, statistical analysis of the sorted populations has been performed using the same concentration in PLTs and RBCs and again a DEP voltage of 10 V_{pp} at 100 kHz. Figure 7 shows the cell count at the different collection channels, obtained by video analysis in the separation region for three different experiments and a total number of 5000 analyzed cells. Those experiments are performed using a flow speed in the separation region around 1 mm/s. The purity obtained at the platelet collection channel is reproducible and very high (98.8%), which is better than the state-of-the-art.[5] Most platelets are

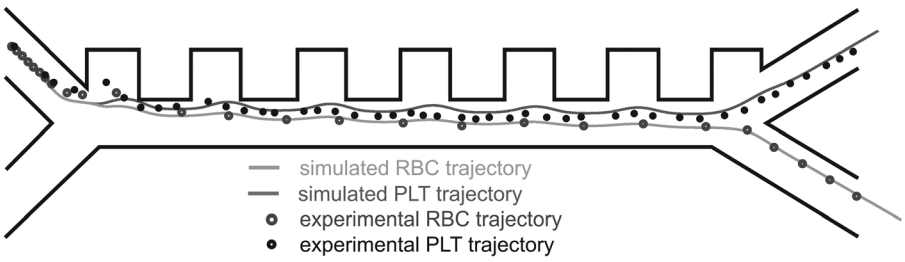

FIG. 6. Graphical representation of the comparison between simulated and experimental trajectories for RBCs and PLTs. The overlap between simulated trajectories (dashed lines) and flowing cells (dots) shows a good agreement between the theory and the experiments.

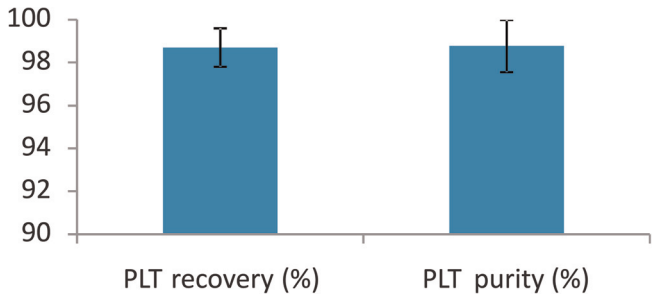

FIG. 7. PLT recovery and purity in the collection channel. These results show the average and standard deviation from three different experiments, with a total number of 5000 analyzed cells (which was only limited by the manual video processing). Both the purity and recovery rates are very high and reproducible, making this platform a robust manner to separate PLTs from blood.

extracted from the sample with over 98% recovery rate, defined as the ratio between the number of platelets collected at the left channel and their total number. The few wrong sorting events are due to the dispersion in cell size among the populations as well as to the cell clusters, mostly present in the red blood cell population.

Platelet activation was not investigated in this work, since care was taken to minimize all the possible activation sources and no evident platelet clumping was observed on-chip. Material-induced activation was prevented as described in Sec. II B using anticoagulants and anti-sticking proteins. Moreover, the electric field intensity was kept one order of magnitude smaller than the state-of-the-art devices described in literature,[5] and the values used to deliberately induced clot formation.[29]

In a control experiment without DEP voltage (not shown here), all cells are going straight to the left collection channel without being deviated, proving that the separation is coming from the applied voltage.

These results prove that the proposed device is robust and able to achieve a very efficient and reproducible separation of platelets with high purity and recovery rates. Its simple technology and low-voltage operation make it possible to adapt the device to a portable platform suitable for point-of-care applications.

V. CONCLUSIONS

We have developed a device able to separate platelets from other blood cells by DEP-FFF. The device uses a combination of flow focusing and dielectrophoresis to separate the cells depending on their size. The electrical field and flow speed have been calculated by numerical simulations. The theoretical cell trajectory can be derived from these simulations, and is in agreement with the experimental results. This method gives a very efficient separation of platelets from other blood cells, yielding high purity and recovery rates. The device can be further integrated with an on-chip cell counter to allow the evaluation of the platelet concentration in the blood. Furthermore, the use of relatively low voltages makes it suitable for point-of-care applications. In a broader perspective, the proposed device can be used to separate other cell types featuring similar differences in size. This sorting principle could also be integrated with a system sorting cells based on their "opacity." Such integration would lead to applications such as complete blood sorting by separating platelets, red blood cells and possibly the different white blood cells by playing both on the cell size difference as on the opacity.

ACKNOWLEDGMENTS

The research leading to these results has received funding from the European Community's Seventh Framework Programme (FP7/2007-2013) under Grant agreement No. 227243. Thanks to the CMI for the access to the cleanroom facilities.

[1]D. F. Stroncek and P. Rebulla, Lancet **370**, 427 (2007).
[2]S. J. Slichter and L. A. Harker, Brit. J. Haematol. **34**, 395 (1976).
[3]H. K. Lin, S. Zheng, A. J. Williams, M. Balic, S. Groshen, H. I. Scher, M. Fleisher, W. Stadler, R. H. Datar, Y.-C. Tai, and R. J. Cote, Clin. Cancer Res. **16**, 5011 (2010).
[4]L. Basabe-Desmonts, S. Ramstrom, G. Meade, S. ONeill, A. Riaz, L. P. Lee, A. J. Ricco, and D. Kenny, Langmuir **26**, 14700 (2010).
[5]M. S. Pommer, Y. Zhang, N. Keerthi, D. Chen, J. A. Thomson, C. D. Meinhart, and H. T. Soh, Electrophoresis **29**, 1213 (2008).
[6]T. Braschler, N. Demierre, E. M. Nascimento, T. Silva, A. G. Oliva, and P. Renaud, Lab Chip **8**, 280 (2008).
[7]G. Mernier, N. Piacentini, R. Tornay, N. Buffi, and P. Renaud, Procedia Chem. **1**, 385 (2009).
[8]G. Mernier, N. Piacentini, R. Tornay, N. Buffi and P. Renaud, Sens. Actuators B **154**, 160 (2011).
[9]G. Mernier, N. Piacentini, and P. Renaud, Lab Chip **10**, 2077 (2010).
[10]G. Mernier, W. Hasenkamp, N. Piacentini, and P. Renaud, Sens. Actuators B (in press).
[11]A. Zeuner, M. Signore, D. Martinetti, M. Bartucci, C. Peschle, and R. De Maria, Cancer Res. **67**, 4767 (2007).
[12]R. Tornay, T. Braschler, N. Demierre, B. Steitz, A. Fink, H. Hofmann, J. A. Hubbell, and P. Renaud, Lab Chip **8** 267 (2008).
[13]N. Demierre, T. Braschler, R. Muller, and P. Renaud, Sens Actuators B **132**, 388 (2008).
[14]T. Braschler, L. Metref, R. Zvitov–Marabi, H. van Lintel, N. Demierre, J. Theytaz, and P. Renaud, Lab Chip **7**, 420 (2007).
[15]N. Demierre, T. Braschler, P. Linderholm, U. Seger, H. van Lintel, and P. Renaud, Lab Chip **7**, 355 (2007).
[16]D. Spiller, P. Losi, E. Briganti, S. Sbrana, S. Kull, I. Martinelli, and G. Soldani, J. Mater. Sci.-Mater. Med. **18**, 1097 (2007).
[17]B. A. Weisenberg and D. L. Mooradian, J. Biomed. Mater. Res. **60**, 283 (2002).
[18]H. G. Gordan, and N. L. Larson, Am. J. Clin. Pathol. **23**, 613 (1955).
[19]C. F. Arkin, D. J. Ernst, A. Marlar, G. T. Parish, D. I. Szamosi, J. D. Wiseman, *NCCLS Document H1-A5* (National committee for clinical laboratory standards, Wayne, PA, USA, 2003).
[20]P. Gascoyne and J. Vykoudal, Electrophoresis **23**, 1973 (2002).
[21]R. Pethig, Biomicrofluidics **4**, 2811 (2010).
[22]P. Gascoyne, J. Satayavivad, and M. Ruchirawat, Acta Trop. **89**, 357 (2004).
[23]M. Egger, E. Donath, P. Spangenberg, M. Bimmler, R. Glasera, and U. Till, BBA–Bioenergetics **972**, 265 (1988).
[24]J. Gimsa, P. Marszaleck, U. Loewe, and T. Tsong, Biophys. J. **60**, 749 (1991).
[25]K. Cheung, S. Gawad, and P. Renaud, Cytometry, Part A **65**, 124 (2005).
[26]D. Holmes, D. Pettigrew, C. H. Reccius, J. D. Gwyer, C. van Berkel, J. Holloway, D. E. Davies, and H. Morgan, Lab Chip **9**, 2881 (2009).
[27]W. van Beaumont, S. Underkofler, and S. van Beaumont, J. Appl. Physiol. **50**, 1255 (1981).
[28]C. Giles, Br. J. Haematol. **48**, 31 (1981).
[29]J. Zhang, P. F. Blackmore, B. Y. Hargrave, S. Xiao, S. J. Beebe, and K. H. Schoenbach, Arch. Biochem. Biophys. **471**, 240 (2008).